Biochimica et Biophysica Acta 1788 (2009) 402–409

Contents lists available at ScienceDirect

Biochimica et Biophysica Acta

journal homepage: www.elsevier.com/locate/bbamem

The high turnover *Drosophila* multidrug resistance-associated protein shares the biochemical features of its human orthologues

Flóra Szeri [a,*], Attila Iliás [a,1], Viola Pomozi [a], Steven Robinow [b], Éva Bakos [a], András Váradi [a]

[a] *Institute of Enzymology, Hungarian Academy of Sciences, Budapest, P.O. Box 7, H-1518, Hungary*
[b] *Department of Zoology, University of Hawaii – Manoa, Honolulu, HI, USA*

ARTICLE INFO

Article history:
Received 16 June 2008
Received in revised form 4 November 2008
Accepted 6 November 2008
Available online 20 November 2008

Keywords:
ABC-transporter
Transport activity
Substrate stimulated-substrate inhibited ATPase activity
Substrate-specificity

ABSTRACT

DMRP, an ABC transporter encoded by the *dMRP/CG6214* gene, is the *Drosophila melanogaster* orthologue of the "long" human multidrug resistance-associated proteins (MRP1/ABCC1, MRP2/ABCC2, MRP3/ABCC3, MRP6/ABCC6, and MRP7/ABCC10). In order to provide a detailed biochemical characterisation we expressed DMRP in Sf9 insect cell membranes. We demonstrated DMRP as a functional orthologue of its human counterparts capable of transporting several human MRP substrates like β-estradiol 17-β-D-glucuronide, leukotriene C_4, calcein, fluo3 and carboxydichlorofluorescein. Unexpectedly, we found DMRP to exhibit an extremely high turnover rate for the substrate transport as compared to its human orthologues. Furthermore, DMRP showed remarkably high basal ATPase activity (68–75 nmol P_i/mg membrane protein/min), which could be further stimulated by probenecid and the glutathione conjugate of N-ethylmaleimide. Surprisingly, this high level basal ATPase activity was inhibited by the transported substrates. We discussed this phenomenon in the light of a potential endogenous substrate (or activator) present in the Sf9 membrane.

1. Introduction

The ATP-binding cassette transporters (ABC transporters), constituting one of the major classes of membrane transporters, have been found ubiquitously in all species studied so far. The majority of these integral membrane proteins utilise the energy of ATP-binding and -hydrolysis to transport substrates across biological membranes [1]. Though some bacterial ABC transporters facilitate the import of nutrients [2], all eukaryote ABC transporters characterised to date transport their substrates from the cytoplasm either to cellular organelles or out of the cell, thus playing essential roles in many cellular processes such as the elimination of endo- and xenobiotics, and the transport of excretory compounds. Besides their physiological relevance, ABC transporters have clinical and economical significance as well, since some confer resistance to antibiotics, chemotherapeutic drugs and herbicides. Of the 48 genes encoding human ABC transporters, 18 have been associated with heritable diseases. [3].

The minimal functional unit of an ABC transporter consists of two transmembrane domains (TMD_1, TMD_2) and two nucleotide binding domains (NBD_1, NBD_2) [4]. These are present – both in human and in *Drosophila* – either as a single protein (full transporters) or as a homo- or heterodimer of two half transporters. Each nucleotide binding domain includes three conserved motifs: the Walker A and B motifs that are commonly observed in ATP binding proteins [5], and the Signature C motif that is unique to ABC transporters [6]. The transmembrane domains TMD1 and TMD2 are composed of six transmembrane helices. A subset of the ABCC subfamily members ("long" MRPs) possesses an additional N-terminal transmembrane domain (TMD_0) – consisting of 5 transmembrane helices – and a large cytoplasmic loop (L_0) connecting TMD_0 to TMD1 [7,8]. This domain organization is characteristic to MRP1, MRP2, MRP3, MRP6, SUR1, SUR2 and MRP7 in humans, while in *Drosophila*, among the 56 ABC proteins, it is present in DSUR and DMRP only [9]. *dSUR* has been identified as the functional orthologue of the mammalian *SUR2* [10,11], coding for the regulatory subunit of the ATP-sensitive potassium (K_{ATP}) channel complex. Recent data suggest that *dSUR* plays a protective role against hypoxic stress and heart failure [12]. The physiological role of *dMRP* has not yet been identified.

A phylogenetic analysis revealed that DMRP is the orthologue of human "long" multidrug resistance-associated proteins MRP1, MRP2, MRP3 and MRP6 [13]. The typical membrane topology of these human MRPs, which was verified experimentally for MRP1

Abbreviations: ABC, ATP-binding cassette; BB, benzbromarone; cAMP, 3′–5′-cyclic adenosine mono-phosphate; CDCF, carboxydichlorofluorescein; CFTR, cystic fibrosis transmembrane conductance regulator; DMRP, *Drosophila* multidrug resistance-associated protein; $E_2$17βDG, β-estradiol 17-β-D-glucuronide; GSH, reduced glutathione; IM, indomethacin; LTC_4, leukotriene C_4; MRP, multidrug resistance-associated protein; NBD, nucleotide binding domain; NEM-GS, N-ethylmaleimide glutathione conjugate; PB, probenecid; SUR, sulfonylurea receptor; Sf9, *Spodoptera frugiperda* ovarian cells; TMD, transmembrane domain; V_i, orthovanadate

* Corresponding author. Tel.: +36 1 2793105; fax: +36 1 4665465.
E-mail address: szeri@enzim.hu (F. Szeri).
[1] Present address: Department of Extracellular Matrix Research, Institute for Biomedical Aging Research, Austrian Academy of Sciences, Innsbruck, Austria.

0005-2736/$ – see front matter © 2008 Elsevier B.V. All rights reserved.
doi:10.1016/j.bbamem.2008.11.007

[14–17], has also been proposed for DMRP previously [13]. The *dMRP/CG6214* gene spans 22 kb of genomic DNA and contains 19 exonic sequences. Nine of them are alternatively spliced for two internally variable exons giving rise to the maximum of fourteen possible transcripts [18]. The existence of different mRNA isoforms, each harbouring 12 exons and all but one coding for transcripts of the same size, was experimentally demonstrated. [18]. Our previous Northern blot and in situ hybridisation analysis, based on the SD07655 *dMRP* clone coding for the 4b 8d isoform confirmed that *dMRP* is expressed in embryonic, larval, pupal, and adult life stages, with enriched expression in the 0–2 h embryos and adult brain [13]. For the biochemical characterisation of the transporter we have expressed DMRP in the Sf9/baculovirus expression system and demonstrated that DMRP is a vanadate-sensitive organic anion transporter, capable of transporting the inflammatory mediator LTC_4, a well-known substrate of the human "long" MRPs [13].

In the present study we provide a comparative analysis of the functional characteristics of DMRP and the human "long" MRPs. Our results indicate that DMRP possesses an unusually high transport capacity for known human MRP substrates. Moreover it exhibits a unique high level basal ATPase activity that is surprisingly inhibited by the transported substrates, however the basal ATPase activity can be further stimulated by the addition of some other compounds. In the discussion section we provide a hypothesis for the above phenomenon.

2. Materials and methods

2.1. Materials

[^{3}H]leukotriene C_4 ([^{3}H]LTC_4; 148 Ci/mmol), and [^{3}H]β-estradiol 17-β-D-glucuronide ([^{3}H]$E_2$17βDG; 48 Ci/mmol) were purchased from PerkinElmer Life Sciences. $^{45}CaCl_2$ (0.8 Ci/mmol) was purchased from Amersham and [^{3}H] cAMP from American Radiolabelled Chemicals, Inc. Calcein, fluo3 and carboxydichlorofluorescein (CDCF) were obtained from Invitrogen — Molecular Probes. Ouabain was purchased from Fluka. The anti-DMRP polyclonal antiserum pAB7655 was raised against a synthetic peptide corresponding to amino acids 209–222 of DMRP (ZYMED Laboratories Inc.) as described [13]. The anti-MRP1 and anti-MRP2 monoclonal antibodies m6 and M_2I-4 were a kind gift of R. Scheper. Secondary HRP-conjugated anti-rabbit and anti-mouse antibodies were purchased from Jackson ImmunoResearch. Nitrocellulose membrane filters (HAWP02500) were obtained from Millipore, and the scintillation fluid (Opti-fluor) from PerkinElmer. All other compounds were obtained from Sigma Aldrich.

2.2. Expression, membrane preparation and immunoblotting

Recombinant baculovirus containing the *dMRP* cDNA (SD07655) coding for isoform 4b 8d was prepared as described previously [13]. MRP1 and MRP2 expression was generated using recombinant baculovirus as described previously [19]. Sf9 cells were cultured and infected with the recombinant baculovirus. After 3-days of virus infection the Sf9 cells were harvested, the membranes were isolated and stored at −70 °C as described by Sarkadi et al. [20]. Total membrane protein concentrations were determined by the modified Lowry method [21]. Gel electrophoresis and immunoblotting were performed as described previously [20] using the anti-DMRP polyclonal antiserum pAB7655 (1:500) or m6 and M_2I-4 (1:10,000). The protein-antibody interaction was visualized by the enhanced chemiluminescence technique (ECL, Amersham Biosciences) using an anti-rabbit (1:10,000) or anti-mouse (1:10,000) horseradish peroxidase-conjugated secondary antibodies. A quantitative measure of expression was determined by densitometry of the immunoblots or gels stained with Coomassie Blue, using Quantity One software (Bio-Rad).

2.3. Vesicular transport measurements

Vesicular transport of radiolabelled substrates were measured using a rapid filtration method [19,22]. Briefly, isolated inside-out Sf9 membrane vesicles containing 100 μg or 2 μg membrane protein (as indicated) were incubated in the presence of 4 mM MgATP or MgAMP in 150 μl of transport buffer (6 mM $MgCl_2$, 40 mM MOPS-Tris, pH 7.0, 40 mM KCl) at 23 °C (LTC_4) or at 37 °C ($E_2$17βDG). Incubation was stopped by the addition of 800 μl of ice-cold washing buffer (40 mM MOPS-Tris, pH 7.0, 70 mM KCl) at the time points indicated. Samples were filtered quickly through 0.45 μm nitrocellulose membrane filters (Millipore). The filters were washed twice with 5 ml of cold washing buffer and the filter-bound radioactivity was measured in scintillation fluid (Opti-fluor, PerkinElmer) using a Wallac 1409 DSA scintillation counter. ATP-dependent transport was calculated by subtracting the activity values obtained in the presence of AMP from those in the presence of ATP. For these experiments, different membrane preparations having a similar proportion of inside-out vesicles were used. The relative amount of uptake-competent inside-out vesicles was determined by measuring the rate of endogenous ATP-dependent $^{45}Ca^{2+}$ uptake of each membrane preparation using a rapid filtration method described previously [22]. Transport values were corrected for non-specific transport observed in the β-galactosidase-expressing control membranes. The Michaelis–Menten kinetic parameters of transport have been determined either from the *x–y* intersections of the Lineweaver–Burk plots or from non-linear regressions of the concentration curves using KaleidaGraph (Synergy Software), as indicated. Data points depicted in the figures show the mean values of at least three independent determinations conducted in duplicates. Error bars depict the standard error of mean value (S.E.M.).

For the fluorescent substrates, vesicular transport measurements were performed on uptake-competent inside-out Sf9 vesicles containing 100 μg membrane protein in the presence of 6 mM MgATP or MgAMP in 100 μl of transport buffer (6 mM $MgCl_2$, 40 mM MOPS-Tris, pH 7.0, 40 mM KCl) at 37 °C at the indicated substrate concentrations, and incubation times. Samples were diluted in PBS (137 mM NaCl, 2.7 mM KCl, 8 mM Na_2HPO_4, 2 mM KH_2PO_4) and a FACSCalibur flow cytometer (Becton-Dickinson, San Jose, CA, USA), equipped with a 488 nm argon-ion laser and a 525 ± 10 nm bandpass filter was used to determine the fluorescence intensity of the dyes accumulated in the membrane vesicles. All data were collected and evaluated by CellQuest software (Becton-Dickinson, San Jose, CA, USA). A total of 10,000 vesicles were counted in each experiment. The geometric mean values of histograms of AMP-containing samples were subtracted from the geometric mean values of histograms of ATP-containing samples, and ATP dependent differences were depicted in the figures. Figures represent at least three independent determinations. The corresponding standard error of mean value (S.E.M.) is depicted.

2.4. ATPase activity measurements

The vanadate-sensitive ATPase activity was measured by colorimetric detection of inorganic phosphate liberation as described previously [19,20]. In brief, membrane suspensions containing 30 μg of membrane protein were incubated at 37 °C for 5 min in 150 μl of a medium containing 40 mM MOPS-Tris, pH 7.0, 0.5 mM EGTA-Tris, 2 mM dithiothreitol, 50 mM KCl, 5 mM sodium azide, and 1 mM ouabain. The ATPase reaction was started by the addition of 3.3 mM MgATP. The indicated drugs were added in DMSO, except for LTC_4 that was diluted in the above assay mix. The final concentration of DMSO in the assay medium was less than 1%. The reactions were stopped by the addition of 0.1 ml of 5% SDS. The amount of inorganic phosphate

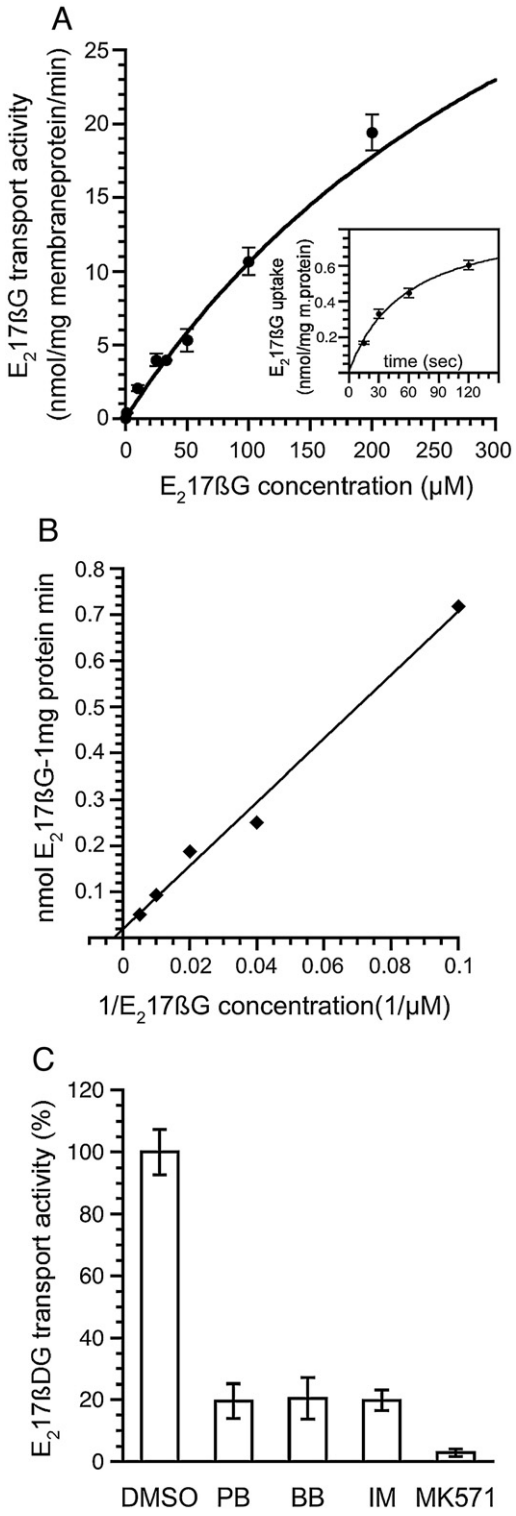

Fig. 1. ATP-dependent $E_2$17βDG uptake into inside-out Sf9 vesicles. Concentration dependence of $E_2$17βDG transport by DMRP at 37 °C for 0.5 min (A). Time-course of the uptake at 1 μM $E_2$17βDG concentration at 37 °C (A inset). Lineweaver–Burk representation of the DMRP mediated $E_2$17βDG transport (B). Inhibition of 0.5 min $E_2$17βDG transport measured at 37 °C and 10 μM $E_2$17βDG concentration in the absence or presence of 2 mM probenecid (PB), 50 μM benzbromarone (BB), 300 μM indomethacin (IM) and 30 μM MK571 (C).

generated was determined based on a colorimetric reaction. The optical density was read at 700 nm after 15 min incubation. ATPase activity was calculated by the difference obtained in P_i levels between 0-min reaction (stopped immediately with SDS) and reactions after the 5-minute incubation periods. The differences between the ATPase activities measured in the absence and presence of 1.33 mM vanadate were taken and activities were corrected for non-specific activity observed in the β-galactosidase-expressing control membranes. Data points depict the mean values of at least three independent determinations conducted in duplicates at a minimum. Error bars depict the standard error of the mean value (S.E.M.).

3. Results

3.1. Transport properties of DMRP

In order to investigate the transport characteristics of DMRP we have expressed the protein in Sf9 insect cells and studied the ATP-dependent uptake of radiolabelled human MRP substrates, the estrogen metabolite β-estradiol 17-β-D-glucuronide ($E_2$17βDG) and the inflammatory mediator leukotriene C_4 (LTC_4) in isolated Sf9 membrane vesicles. The initial linear phase of the transport was determined and the ATP-dependent transport values were corrected with the almost negligible uptake measured in β-galactosidase expressing control Sf9 membranes.

As demonstrated in the inset of Fig. 1A, at 37 °C, DMRP-dependent transport of 1 μM $E_2$17βDG provided a good approximation of the initial transport rate at 30 s. Therefore, these conditions were used to study the concentration dependent uptake of $E_2$17βDG (Fig. 1A). The kinetic parameters of transport were determined from the Lineweaver–Burk plot (Fig. 1B). The apparent K_m value was found to be 344 ± 182 μM and the maximum rate of transport was 50 ± 25 nmol/mg of membrane protein/min. Due to the low solubility of the compound, the concentration dependence at higher concentrations could not be measured. Therefore these kinetic parameters have to be considered as best estimates.

We found DMRP to exhibit an extremely high turnover rate for LTC_4 transport. To measure initial velocity, we reduced the amount of vesicles 50 times to 2 μg total membrane protein/sample, and measured LTC_4 transport of DMRP at 23 °C. In comparison, MRP1-dependent LTC_4 transport was measured at 37 °C in vesicles containing 100 μg total membrane protein/sample. In control experiments we measured the transport activity values of mixed vesicle preparations (using 10 μg DMRP, and 90 μg β-galactosidase or 1 μg DMRP and 9 μg β-galactosidase vesicles), in parallel with 10 μg or 1 μg vesicles exclusively overexpressing DMRP. We obtained similar results for the mixed vesicle controls and the vesicles expressing DMRP (results not shown), suggesting that the dramatic reduction of the vesicular content did not result in unspecific changes. Therefore, we performed the experiments on 2 μg total membrane protein containing vesicles obtained from DMRP over-expressing Sf9 cells. The time-course of LTC_4 uptake in 2 μg isolated vesicles at 23 °C, 50 nM LTC_4 is demonstrated in the left-hand-side inset of Fig. 2A. Kinetic parameters of DMRP-mediated LTC_4 transport were determined at 30 s, while for MRP1 we used the generally accepted conditions reflecting the initial rate of transport (100 μg protein, 23 °C, 30 s). The uptake was a saturable function of the LTC_4 concentration for both DMRP and MRP1 (Fig. 2A). We calculated the kinetic parameters from the Lineweaver–Burk plots (Fig. 2B) as the maximum uptake rates of 3038 ± 666 pmol/mg of membrane protein/min and 73 ± 15 pmol/mg of membrane protein/min; and the apparent K_m values of 231 ± 60 nM and 187 ± 47 nM for DMRP and MRP1, respectively. The vesicles contained similar amounts of over-expressed proteins as detected by Coomassie staining (data not shown).

We also investigated the effect of known human MRP inhibitors on the $E_2$17βDG and LTC_4 transport. The organic anions probenecid (PB), benzbromarone (BB), indomethacin (IM), and the leukotriene receptor antagonist MK571 effectively inhibited both $E_2$17βDG and LTC_4 transport of DMRP (Figs. 1C and 2C) in a concentration range relevant for the "long" human orthologues [19,23,24].

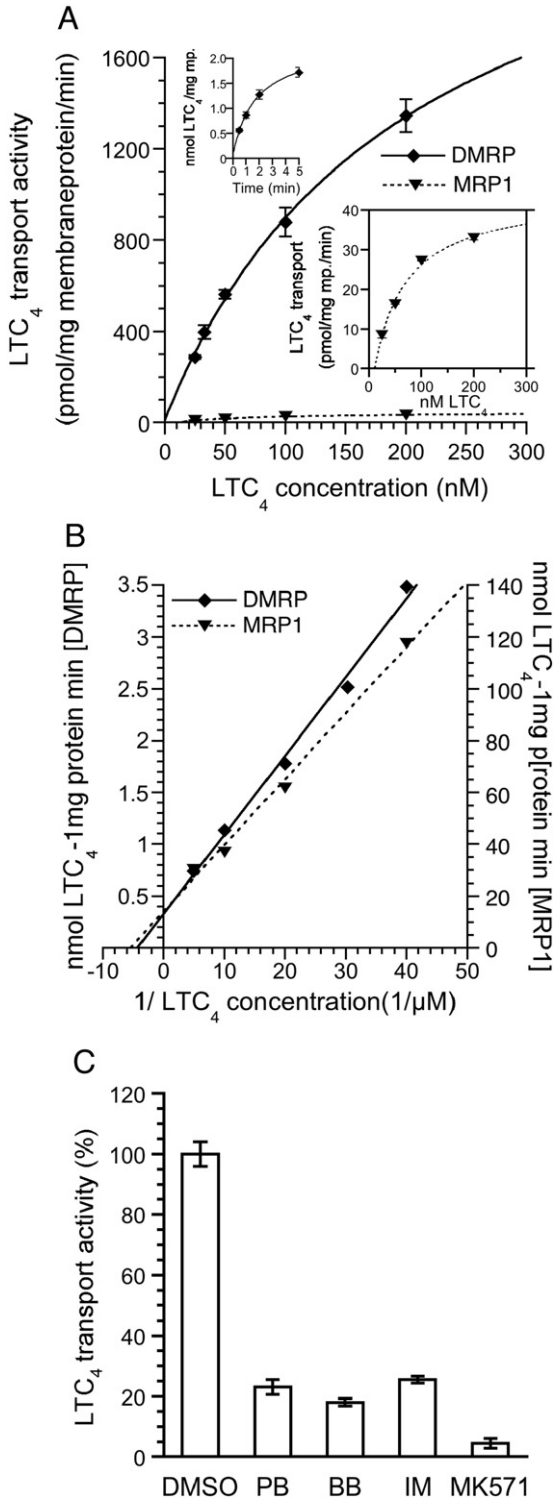

Fig. 2. ATP-dependent LTC_4 uptake into inside-out Sf9 vesicles. Experiments were performed at 23 °C for 0.5 min on either 2 or 100 μg of total protein containing membrane prepared from DMRP or MRP1 overexpressing Sf9 cells, respectively. Concentration dependence of the DMRP and MRP1 mediated LTC_4 transport (A). Time-course of DMRP-dependent LTC_4 uptake at 50 nM LTC_4 concentration (A inset1). Re-plot of the MRP1-dependent LTC_4 uptake depicted in panel A (A inset 2). Lineweaver–Burk representation of the DMRP and MRP1 mediated LTC_4 transport (B). Inhibition of DMRP dependent LTC_4 transport performed at 10 nM LTC_4 concentration for 0.5 min in the absence or presence of 2 mM probenecid (PB), 50 μM benzbromarone (BB), 300 μM indomethacin (IM) and 30 μM MK571 (C).

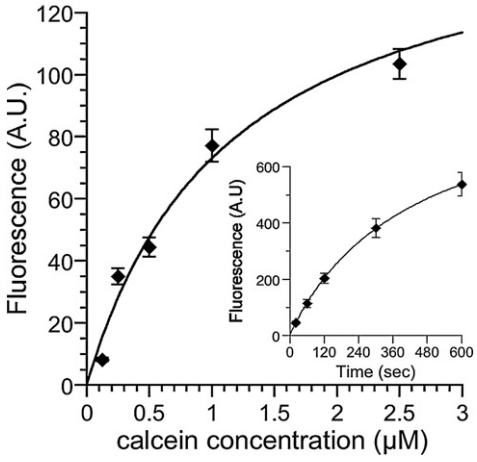

Fig. 3. ATP-dependent uptake of calcein into inside-out Sf9 vesicles. Experiments were performed on 100 μg of total protein containing Sf9 vesicles prepared from DMRP overexpressing cells. The geometric means of the ATP dependent fluorescence intensity values of 10,000 vesicles incubated at 37 °C for 0.5 min are depicted. Main figure shows the fluorescence intensity as a function of calcein concentration. Inset depicts the time-course of calcein uptake at 1 μM calcein concentration.

We investigated the ability of DMRP to transport [^{3}H] 3′–5′-cyclic adenosine mono-phosphate (cAMP), substrate of the short MRPs (MRP4 [25] and MRP5 [26]), as well. We used 100 μg transport competent vesicles at 37 °C at the concentration of 10–100 μM cAMP for 10 minute incubation. In parallel we tested the LTC_4 transport activity of DMRP to monitor DMRP-function. We didn't detect any ATP dependent transport of cAMP, suggesting that cAMP is not a substrate for DMRP.

We used flow cytometry to test the ability of DMRP to transport fluorescent human MRP substrates. We investigated the DMRP, MRP1 and MRP2 dependent uptake of calcein, Fluo3, and carboxydichloro-fluorescein (CDCF) at 37 °C, in the presence of 6 mM MgATP or MgAMP. We measured the uptake of the fluorescent substrates as a function of the incubation time, and used incubation times within the linear range to determine the kinetic parameters of the transports. Due to the lack of calibration, the apparent V_{max} values, always determined under identical experimental conditions, are only arbitrary units suitable for representing turnover differences of the transporters. Coomassie staining revealed that the vesicles investigated in FACS measurements all contained similar amount of over-expressed proteins (data not shown).

In case of calcein we could only detect DMRP-dependent transport activity, possibly due to the relatively low sensitivity of the assay. Time-course showed approximate linearity up to 60 s at 37 °C (Fig. 3 inset), therefore we used these conditions to measure transport activity as a function of calcein concentration (Fig. 3). We determined the apparent K_m of the calcein transport as 1.15±0.17 μM for DMRP applying non-linear regression of the concentration curve.

For fluo3 we could detect significant transport activity for DMRP and MRP2, but not for MRP1. Time-course for fluo3 showed approximate linearity up to 0.5 and 1 min for DMRP and MRP2 at 37 °C, respectively (Fig. 4A), and these conditions were used to determine the apparent kinetic parameters (Fig. 4B). We determined the K_m values for DMRP and MRP2 from non-linear regression of the concentration curve. The apparent K_m values are 0.37±0.13 μM for DMRP and 0.81±0.40 μM for MRP2. The difference between the arbitrary turnover rates determined in the same experiments for DMRP and MRP2 was remarkable. We detected 8.4 times higher activity for DMRP than for MRP2, while the vesicles contained similar amounts of overexpressed proteins (data not shown).

In case of CDCF, the DMRP-dependent dye accumulation was prominent, while a moderate activity was detected for MRP2 and a

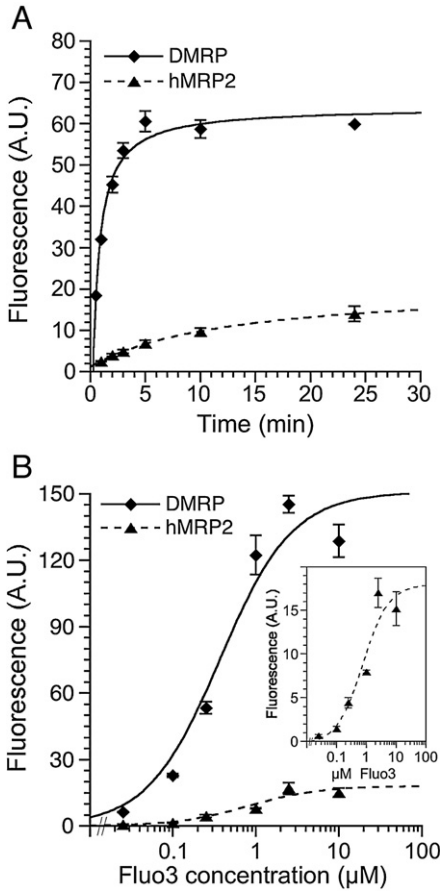

Fig. 4. ATP-dependent uptake of fluo3 into inside-out Sf9 vesicles. Experiments were performed on 100 μg of total protein containing Sf9 vesicles either prepared from DMRP or MRP2 overexpressing cells. The geometric mean values of the ATP dependent fluorescent intensities of 10,000 vesicles incubated at 37 °C are depicted. Time-course of fluo3 uptake at 0.5 μM substrate concentration (A). Fluorescence intensity as a function of fluo3 concentration incubated for 0.5 min for DMRP and 1 min for MRP2, data corrected for incubation time (B). Re-plot of the MRP2-dependent transport activity (B, inset).

threshold level of transport activity for MRP1. Therefore we only investigated the activity of the aforementioned two transporters. Time-course showed approximate linearity at 37 °C up to 0.5 and 1 min for DMRP and MRP2, respectively (Fig. 5 inset). Therefore these conditions were applied to determine kinetic parameters of the CDCF transport (Fig. 5). Since we detected an unspecific ATP independent effect of CDCF on the transport assay above 50 μM CDCF concentration, we only used and presented data up to 25 μM CDCF concentrations. This interval included the effective concentration range of CDCF for DMRP but not for MRP2. Therefore applying non-linear regression we could only determine the K_m values of the DMRP dependent transport as 4.1 ± 0.6 μM CDCF.

The ATP-dependent tracer uptake of the β-galactosidase control membranes showed negligible background transport activity for the three fluorescent substrates (data not shown).

The MRP specific inhibitor MK571 effectively inhibited the accumulation of calcein, fluo3 and CDCF in DMRP over-expressing Sf9 vesicles at a concentration of 30 μM (data not shown).

3.2. The ATPase activity of DMRP; effect of substrates and inhibitors

Transported substrates of ABC-transporters are known to influence ATPase activity most commonly by increasing the rate of ATP hydrolysis (substrate-stimulated ATPase activity) [20]. To investigate the interaction between the substrates and the transporter we characterised the ATPase activity of the transporter in the absence or in the presence of different compounds (Fig. 6). The vanadate-sensitive basal and 5 mM NEM-GS stimulated ATPase activities of DMRP were found to show approximate linearity up to 5 min at 37 °C and 3.3 mM Mg^{2+}ATP concentration (Fig. 6A). As depicted in Fig. 6B, both vanadate-sensitive basal and 5 mM NEM-GS stimulated activities were saturated above 2 mM Mg^{2+}ATP concentration. To further characterise the ATPase activity of the transporter we investigated its vanadate-sensitive ATPase activity in response to NEM-GS, probenecid, LTC_4, and $E_217\beta DG$ (Fig. 6C). Control membranes from cells expressing β-galactosidase had a low level basal ATPase activity (5–8 nmol P_i/mg of membrane protein/min) independent of the presence of the tested compounds (data not shown). The vanadate-sensitive ATPase activity of DMRP in the absence of any substrate was unusually high (68–75 nmol P_i/mg of membrane protein/min) compared to that of human MRP1 (6–8 nmol P_i/mg of membrane protein/min), [19,23]. The basal activity could be stimulated 1.9 fold in the presence of the synthetic glutathione-conjugate, NEM-GS (2.5 mM), and 1.8 fold in the presence of the organic anion probenecid (1 mM) (Fig. 6C). Interestingly, all of the investigated DMRP transport substrates (LTC_4, calcein, and $E_217\beta DG$) inhibited the basal ATPase activity. The inhibited (residual) activity was 46% for LTC_4, 77% for calcein (data not shown) and 12.5% for $E_217\beta DG$, at the highest concentrations used (Fig. 6C). The IC_{50} values for LTC_4 and $E_217\beta DG$ in ATPase activity measurements correlated well with the apparent K_m values determined in the transport experiments. The specific MRP inhibitor MK571 inhibited both the NEM-GS stimulated and the basal ATPase activity in a concentration dependent manner with IC_{50} values of 1.05 and 2.05 μM, respectively (Fig. 6D).

4. Discussion

The present study focused on a detailed characterisation of DMRP, the only *Drosophila melanogaster* orthologue of the human "long" MRPs (MRP1, 2, 3, 6, and 7), providing an analysis of *Drosophila* MRP transport and ATPase activities by comparing them to those of its human orthologues.

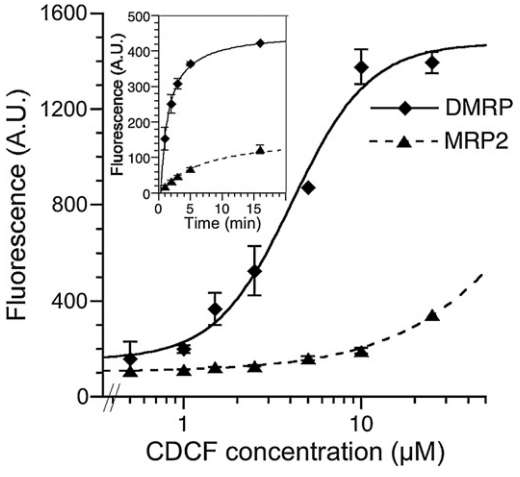

Fig. 5. ATP-dependent uptake of CDCF (carboxydichlorofluorescein) into inside-out Sf9 vesicles. Experiments were performed on 100 μg of total protein containing Sf9 vesicles either prepared from DMRP or MRP2 overexpressing cells. The geometric mean values of the ATP dependent fluorescence intensity values of 10,000 vesicles incubated at 37 °C are shown. Main figure shows the fluorescence intensity as a function of CDCF concentration incubated for 0.5 and 1 min for DMRP and MRP2, respectively. (Data has been corrected for incubation time). Time-course of CDCF uptake at 2.5 μM concentration (inset).

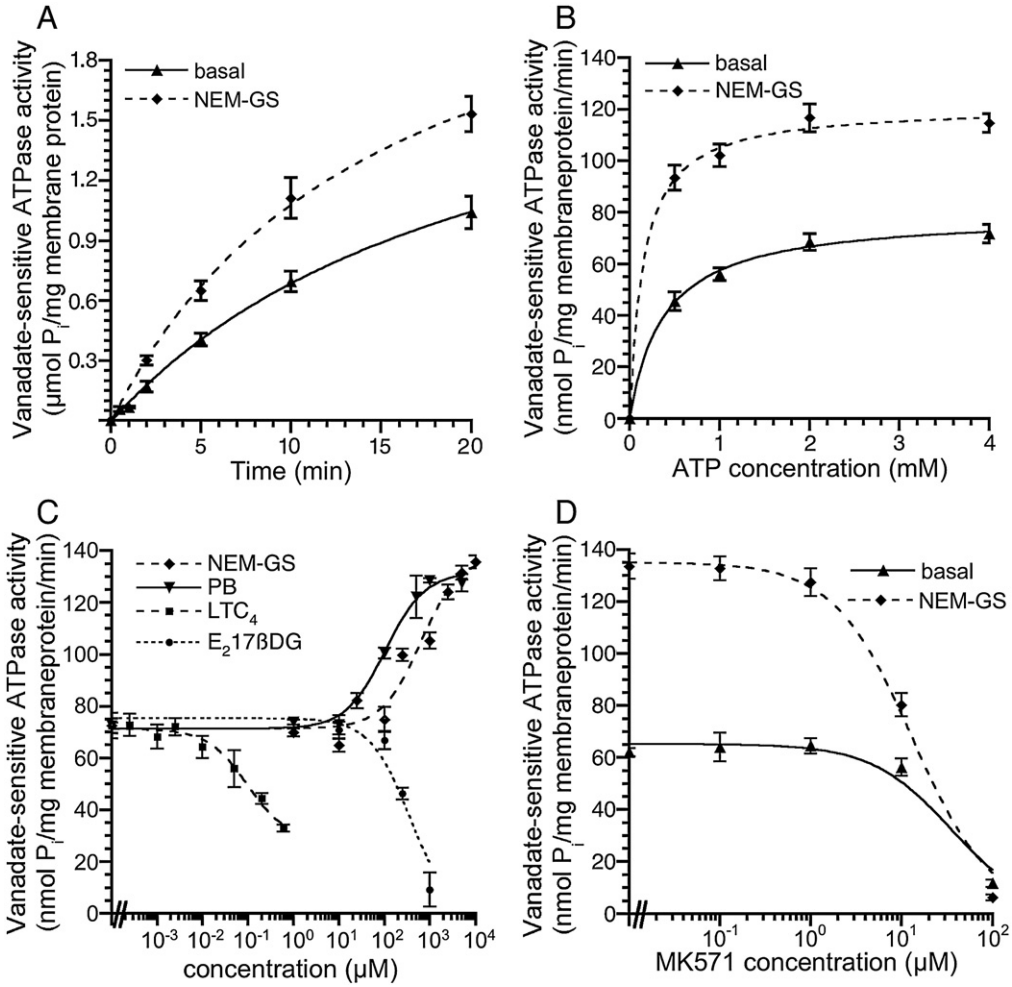

Fig. 6. Effect of modulators on the vanadate-sensitive ATPase activity of DMRP. Time-course of the vanadate-sensitive ATPase activity of DMRP at 37 °C and 3.3 mM Mg^{2+}ATP concentration in the presence or absence of 5 mM NEM-GS (A). Mg^{2+}ATP concentration dependence of the vanadate-sensitive ATPase activity of DMRP at 37 °C incubated for 5 min in the presence or absence of 5 mM NEM-GS (B). DMRP dependent vanadate-sensitive ATPase activity at 37 °C, 3.3 mM Mg^{2+}ATP concentration incubated for 5 min in the absence or presence of various concentration of the following compounds: NEM-GS (diamond), probenecid (triangle), LTC_4 (square), $E_2$17βDG (circle) (C). DMRP-dependent vanadate-sensitive ATPase activity as a function of MK571 concentration in the absence (triangle) or in the presence (diamond) of 5 mM NEM-GS (D).

For such a comparative investigation proteins were expressed in the Sf9/baculovirus expression system and the ability of DMRP to transport different human MRP substrates, such as $E_2$17βDG, LTC_4, calcein, fluo3 and CDCF were tested in vesicular transport experiments.

Human "long" MRPs were shown to transport $E_2$17βDG [27–33]. The majority of these proteins show modest capacity but low K_m values (apparent K_m of 10–70 µM) for $E_2$17βDG with the exception of MRP2, which shows high K_m value but is considered to have the highest transport rate for this substrate [34]. We detected 4.6 times higher maximal transport rate for DMRP than for MRP2 in the $E_2$17βDG vesicular transport experiments, while the expression level of DMRP in vesicles used for determination of $E_2$17βDG transport kinetic parameters was approximately one-fourth of the expression of MRP2. Therefore the maximal transport rate of DMRP is approximately 18 times higher than that of MRP2. We found that the K_m of DMRP for this substrate is relatively high, therefore we consider DMRP as a unique high capacity transporter of $E_2$17βDG, resembling the properties of MRP2, as both transporters show high K_m and transport rate values.

All "long" MRPs are capable of transporting LTC_4 with different transport characteristics [24,29,31,32,35]. We have investigated the LTC_4 transport properties of DMRP, and found the maximal transport rate of DMRP for LTC_4 approximately 40 times higher than that of the physiologically relevant MRP1, while DMRP possesses slightly higher K_m value for LTC_4 than MRP1.

It was previously shown that MRP1 is capable of transporting calcein [36], while fluo3 is transported by both MRP1 and MRP2 [37–39]. CDCF was proven to be a substrate for MRP2 and MRP5 [40]. We investigated the ability of DMRP to transport these fluorescent substrates of the human MRPs, and determined their apparent K_m values. We detected a high turnover rate for DMRP for all the three fluorescent substrates, while MRP2 investigated in parallel showed only moderate transport activity for fluo3 and CDCF (though these transporters were expressed at similar levels).

We investigated the inhibitor profile of the DMRP-dependent transport and found that the organic anions probenecid, benzbromarone, indomethacin, and the leukotriene receptor antagonist MK571 exhibited potent inhibitory effects on DMRP transport at concentrations that negatively impact the transport properties of the human orthologues as well [19,22–24,34].

The ATPase activity measurements showed that DMRP has the highest basal activity (68–75 nmol P_i/mg membrane protein/min) of any MRP studied to date in Sf9 membrane vesicle preparations [19,23]. This unusually high basal activity of DMRP could be further stimulated by NEM-GS and probenecid. Surprisingly, all of the investigated DMRP transport substrates inhibited the basal ATPase activity in a

concentration dependent manner for the whole effective concentration range (Fig. 6C).

Collectively, these observations demonstrate that DMRP reflects many properties of the human "long" MRPs including substrate and inhibitor specificity. However, there are several unique features of DMRP revealed by the present study: i) compared to the human transporters, DMRP exhibits a much higher transport activity; ii) DMRP has an unusually high basal ATPase activity; iii) the investigated DMRP substrates inhibit the basal ATPase activity.

The remarkable activity of DMRP compared to that of the human transporters may partially originate from the fact that it is an insect protein expressed in a similar host cell. In addition, we hypothesise that DMRP in the Sf9 membrane is already in an activated state. This could either originate from the presence of endogenous substrate(s) or activator molecule(s) characteristic of Sf9 cells. This activation is presumably not complete, since NEM-GS and probenecid can evoke further activation of the ATPase activity. Nevertheless, this partial activation would imply that the transporter efficiently hydrolyses ATP even in the absence of any external substrate, though an external substrate may successfully compete with the endogenous activator. If such a competitive external substrate is added and the potential of the external substrate to trigger ATP hydrolysis is weaker than that of the endogenous one, an apparent inhibition of the ATPase activity may be detected. Investigations of purified DMRP reconstituted in different membrane environments would shed light onto the relevance of the above hypothesis. The work aiming to obtain active purified protein is on the way.

Another question is whether the high basal activity detected in vitro has any relevance in vivo. It is quite unlikely that an organism would pay the cost for having such an ATP depleting active transporter unless it had a fundamental role in its homeostasis. Since DMRP knock out animals are viable and fertile (http://flybase.org, FlyBase ID: FBti0024660, FBti0057681) and dMRP cDNA is present ubiquitously [13], it seems that this is not the case. It is more likely that DMRP does not possess such a high basal activity in its natural environment, e.g., due to the lack of such an activator or the presence of some negative regulatory mechanisms.

The present article provides information on the characteristics of DMRP revealing that DMRP possesses combined features of its human orthologues, however exhibiting a remarkably higher activity. These features make DMRP a valuable model protein for further studies to reveal the mechanistic features of MRPs, especially for investigations that require high turnover.

Acknowledgements

This work was supported by the OTKA NI68950 and NK48729 grants to A. Váradi, and NF61822 grant for É. Bakos by the Hungarian Scientific Research Fund and grants from the Victoria S. and Bradley L. Geist Foundation to S. Robinow. We are grateful to K. Liliom for many valuable discussions and critical reading of the manuscript. We thank R. Scheper and M. Flens for providing hMRP1 and hMRP2 monoclonal antibodies.

References

[1] I.B. Holland, M.A. Blight, ABC-ATPases, adaptable energy generators fuelling transmembrane movement of a variety of molecules in organisms from bacteria to humans, J. Mol. Biol. 293 (1999) 381–399.
[2] C.F. Higgins, ABC transporters: physiology, structure and mechanism—an overview, Res. Microbiol. 152 (2001) 205–210.
[3] M. Dean, T. Annilo, Evolution of the ATP-binding cassette (ABC) transporter superfamily in vertebrates, Annu. Rev. Genomics Hum. Genet. 6 (2005) 123–142.
[4] C.F. Higgins, I.D. Hiles, G.P. Salmond, D.R. Gill, J.A. Downie, I.J. Evans, I.B. Holland, L. Gray, S.D. Buckel, A.W. Bell, et al., A family of related ATP-binding subunits coupled to many distinct biological processes in bacteria, Nature 323 (1986) 448–450.
[5] J.E. Walker, M. Saraste, M.J. Runswick, N.J. Gay, Distantly related sequences in the alpha- and beta-subunits of ATP synthase, myosin, kinases and other ATP-requiring enzymes and a common nucleotide binding fold, EMBO J. 1 (1982) 945–951.
[6] S.C. Hyde, P. Emsley, M.J. Hartshorn, M.M. Mimmack, U. Gileadi, S.R. Pearce, M.P. Gallagher, D.R. Gill, R.E. Hubbard, C.F. Higgins, Structural model of ATP-binding proteins associated with cystic fibrosis, multidrug resistance and bacterial transport, Nature 346 (1990) 362–365.
[7] G.E. Tusnady, E. Bakos, A. Varadi, B. Sarkadi, Membrane topology distinguishes a subfamily of the ATP-binding cassette (ABC) transporters, FEBS Lett. 402 (1997) 1–3.
[8] I. Klein, B. Sarkadi, A. Varadi, An inventory of the human ABC proteins, Biochim. Biophys. Acta 1461 (1999) 237–262.
[9] M. Dean, A. Rzhetsky, R. Allikmets, The human ATP-binding cassette (ABC) transporter superfamily, Genome Res. 11 (2001) 1156–1166.
[10] I. Nasonkin, A. Alikasifoglu, C. Ambrose, P. Cahill, M. Cheng, A. Sarniak, M. Egan, P.M. Thomas, A novel sulfonylurea receptor family member expressed in the embryonic *Drosophila* dorsal vessel and tracheal system, J. Biol. Chem. 274 (1999) 29420–29425.
[11] S.K. Kim, E.J. Rulifson, Conserved mechanisms of glucose sensing and regulation by *Drosophila* corpora cardiaca cells, Nature 431 (2004) 316–320.
[12] T. Akasaka, S. Klinedinst, K. Ocorr, E.L. Bustamante, S.K. Kim, R. Bodmer, The ATP-sensitive potassium (KATP) channel-encoded dSUR gene is required for *Drosophila* heart function and is regulated by tinman, Proc. Natl. Acad. Sci. U. S. A. 103 (2006) 11999–12004.
[13] J.N. Tarnay, F. Szeri, A. Ilias, T. Annilo, C. Sung, O. Le Saux, A. Varadi, M. Dean, C.D. Boyd, S. Robinow, The dMRP/CG6214 gene of *Drosophila* is evolutionarily and functionally related to the human multidrug resistance-associated protein family, Insect Mol. Biol. 13 (2004) 539–548.
[14] E. Bakos, T. Hegedus, Z. Hollo, E. Welker, G.E. Tusnady, G.J. Zaman, M.J. Flens, A. Varadi, B. Sarkadi, Membrane topology and glycosylation of the human multidrug resistance-associated protein, J. Biol. Chem. 271 (1996) 12322–12326.
[15] D.R. Hipfner, K.C. Almquist, E.M. Leslie, J.H. Gerlach, C.E. Grant, R.G. Deeley, S.P. Cole, Membrane topology of the multidrug resistance protein (MRP). A study of glycosylation-site mutants reveals an extracytosolic NH2 terminus, J. Biol. Chem. 272 (1997) 23623–23630.
[16] C. Kast, P. Gros, Topology mapping of the amino-terminal half of multidrug resistance-associated protein by epitope insertion and immunofluorescence, J. Biol. Chem. 272 (1997) 26479–26487.
[17] C. Kast, P. Gros, Epitope insertion favors a six transmembrane domain model for the carboxy-terminal portion of the multidrug resistance-associated protein, Biochemistry 37 (1998) 2305–2313.
[18] M. Grailles, P.T. Brey, C.W. Roth, The *Drosophila melanogaster* multidrug-resistance protein 1 (MRP1) homolog has a novel gene structure containing two variable internal exons, Gene 307 (2003) 41–50.
[19] E. Bakos, R. Evers, E. Sinko, A. Varadi, P. Borst, B. Sarkadi, Interactions of the human multidrug resistance proteins MRP1 and MRP2 with organic anions, Mol. Pharmacol. 57 (2000) 760–768.
[20] B. Sarkadi, E.M. Price, R.C. Boucher, U.A. Germann, G.A. Scarborough, Expression of the human multidrug resistance cDNA in insect cells generates a high activity drug-stimulated membrane ATPase, J. Biol. Chem. 267 (1992) 4854–4858.
[21] A. Bensadoun, D. Weinstein, Assay of proteins in the presence of interfering materials, Anal. Biochem. 70 (1976) 241–250.
[22] E. Bakos, R. Evers, G. Szakacs, G.E. Tusnady, E. Welker, K. Szabo, M. de Haas, L. van Deemter, P. Borst, A. Varadi, B. Sarkadi, Functional multidrug resistance protein (MRP1) lacking the N-terminal transmembrane domain, J. Biol. Chem. 273 (1998) 32167–32175.
[23] A. Bodo, E. Bakos, F. Szeri, A. Varadi, B. Sarkadi, The role of multidrug transporters in drug availability, metabolism and toxicity, Toxicol. Lett. 140–141 (2003) 133–143.
[24] A. Ilias, Z. Urban, T.L. Seidl, O. Le Saux, E. Sinko, C.D. Boyd, B. Sarkadi, A. Varadi, Loss of ATP-dependent transport activity in pseudoxanthoma elasticum-associated mutants of human ABCC6 (MRP6), J. Biol. Chem. 277 (2002) 16860–16867.
[25] Z.S. Chen, K. Lee, G.D. Kruh, Transport of cyclic nucleotides and estradiol 17-beta-D-glucuronide by multidrug resistance protein 4. Resistance to 6-mercaptopurine and 6-thioguanine, J. Biol. Chem. 276 (2001) 33747–33754.
[26] G. Jedlitschky, B. Burchell, D. Keppler, The multidrug resistance protein 5 functions as an ATP-dependent export pump for cyclic nucleotides, J. Biol. Chem. 275 (2000) 30069–30074.
[27] G. Jedlitschky, I. Leier, U. Buchholz, K. Barnouin, G. Kurz, D. Keppler, Transport of glutathione, glucuronate, and sulfate conjugates by the MRP gene-encoded conjugate export pump, Cancer Res. 56 (1996) 988–994.
[28] D.W. Loe, K.C. Almquist, S.P. Cole, R.G. Deeley, ATP-dependent 17 beta-estradiol 17-(beta-D-glucuronide) transport by multidrug resistance protein (MRP). Inhibition by cholestatic steroids, J. Biol. Chem. 271 (1996) 9683–9689.
[29] Y. Cui, J. Konig, J.K. Buchholz, H. Spring, I. Leier, D. Keppler, Drug resistance and ATP-dependent conjugate transport mediated by the apical multidrug resistance protein, MRP2, permanently expressed in human and canine cells, Mol. Pharmacol. 55 (1999) 929–937.
[30] N. Zelcer, T. Saeki, G. Reid, J.H. Beijnen, P. Borst, Characterization of drug transport by the human multidrug resistance protein 3 (ABCC3), J. Biol. Chem. 276 (2001) 46400–46407.
[31] H. Zeng, G. Liu, P.A. Rea, G.D. Kruh, Transport of amphipathic anions by human multidrug resistance protein 3, Cancer Res. 60 (2000) 4779–4784.
[32] Z.S. Chen, E. Hopper-Borge, M.G. Belinsky, I. Shchaveleva, E. Kotova, G.D. Kruh, Characterization of the transport properties of human multidrug resistance protein 7 (MRP7, ABCC10), Mol. Pharmacol. 63 (2003) 351–358.
[33] M.G. Belinsky, Z.S. Chen, I. Shchaveleva, H. Zeng, G.D. Kruh, Characterization of the drug resistance and transport properties of multidrug resistance protein 6 (MRP6, ABCC6), Cancer Res. 62 (2002) 6172–6177.
[34] A. Bodo, E. Bakos, F. Szeri, A. Varadi, B. Sarkadi, Differential modulation of the human liver conjugate transporters MRP2 and MRP3 by bile acids and organic anions, J. Biol. Chem. 278 (2003) 23529–23537.
[35] I. Leier, G. Jedlitschky, U. Buchholz, S.P. Cole, R.G. Deeley, D. Keppler, The MRP gene

encodes an ATP-dependent export pump for leukotriene C4 and structurally related conjugates, J. Biol. Chem. 269 (1994) 27807–27810.
[36] N. Feller, H.J. Broxterman, D.C. Wahrer, H.M. Pinedo, ATP-dependent efflux of calcein by the multidrug resistance protein (MRP): no inhibition by intracellular glutathione depletion, FEBS Lett. 368 (1995) 385–388.
[37] D. Keppler, Y. Cui, J. Konig, I. Leier, A. Nies, Export pumps for anionic conjugates encoded by MRP genes, Adv. Enzyme Regul. 39 (1999) 237–246.
[38] F. Kyle-Cezar, E.-L.J. dos Santos, R.C. Goldenberg, V.M. Rumjanek, Expression of c-kit and Sca-1 and their relationship with multidrug resistance protein 1 in mouse bone marrow mononuclear cells, Immunology 121 (2007) 122–128.
[39] A.T. Nies, T. Cantz, M. Brom, I. Leier, D. Keppler, Expression of the apical conjugate export pump, Mrp2, in the polarized hepatoma cell line, WIF-B, Hepatology 28 (1998) 1332–1340.
[40] S. Pratt, V. Chen, W.I. Perry III, J.J. Starling, A.H. Dantzig, Kinetic validation of the use of carboxydichlorofluorescein as a drug surrogate for MRP5-mediated transport, Eur. J. Pharm. Sci. 27 (2006) 524–532.